Desalination and Water Treatment
www.deswater.com

doi: 10.1080/19443994.2015.1041056

57 (2016) 10941–10947
May

Preparation and characterization of Zr and Sn doped TiO_2 nanocomposite and photocatalytic activity in degradation of tetracycline

H.R. Pouretedal[a,*], B. Afshari[b]

[a]*Faculty of Applied Chemistry, Malek-Ashtar University of Technology, Shahin-Shahr, Iran, Tel. +98 314 591 2253; email: HR_POURETEDAL@mut-es.ac.ir*
[b]*Department of Chemistry, Islamic Azad University, Shahreza Branch, Shahreza, Iran, Tel. +98 315 329 2222; email: afshari248@yahoo.com*

Received 23 October 2014; Accepted 29 March 2015

ABSTRACT

The photocatalysts of $Ti_{0.9}Zr_{0.03}Sn_{0.07}O_2$, $Ti_{0.9}Zr_{0.05}Sn_{0.05}O_2$, and $Ti_{0.9}Zr_{0.07}Sn_{0.03}O_2$ nanocomposite were prepared using the sol–gel method. The structure of anatase–rutile for prepared photocatalysts was confirmed using X-ray diffraction patterns. The transmission electron microscope image indicated that the size of nanoparticles was in range of 30–80 nm. The elemental analysis of $Ti_{0.9}Zr_{0.05}Sn_{0.05}O_2$ nanocomposite was confirmed by energy dispersive X-ray analysis. The UV–vis absorbance spectra of nanocomposites showed a red-shift of band-gap energies of semiconductors vs. TiO_2 pure nanoparticles. The application of prepared nanophotocatalysts was studied in tetracycline photodegradation in aqueous samples. The complete degradation of pollutant in a photodegradation reaction with rate constant of 27.0×10^{-3} min^{-1} was obtained at optimized conditions of 0.8 g/L of $Ti_{0.9}Zr_{0.05}Sn_{0.05}O_2$, pH 3, 20.0 mg/L of tetracycline and during time 180 min. The photocatalytic activity of nanoparticles was seen as $Ti_{0.9}Zr_{0.05}Sn_{0.05}O_2 > Ti_{0.9}Zr_{0.07}Sn_{0.03}O_2 > Ti_{0.9}Zr_{0.03}Sn_{0.07}O_2 > TiO_2$ that is related to the band-gap energies as $2.95 < 2.99 < 3.22 < 3.28$ eV, respectively. The reusability of $Ti_{0.9}Zr_{0.05}Sn_{0.05}O_2$ photocatalyst was tested in four cycles of photodegradation process. The resistance against of photocorrosion is due to reproducibility of photocatalytic activity.

Keywords: Nanocomposite; Photocatalyst; TiO_2; Tetracycline; Photodegradation

1. Introduction

In the last decades, heterogeneous photocatalysis as an effective technique has received great attention for the purification of polluted air and wastewater [1,2]. The photocatalysis is based upon the use of UV–vis irradiated semiconductors, such as titanium dioxide (TiO_2), to destroy various organic pollutants such as wastewater of drugs. TiO_2 has been extensively studied for environmental purification applications, due to its good photocatalytic activity, high stability, non-toxicity, and non-biodegradability. Moreover, it is a semiconductor under the form of thin films and dispersed nanoparticles. Insensitivity of TiO_2 to visible light is related to its band-gap (3.2 eV) that enables it to absorb in the near ultraviolet region, even though its low efficiency [3,4].

The synthesis of the new nanocomposites, the mixed photocatalysts andf doping of photocatalysts

---

*Corresponding author.

with metal and non-metal elements are used to increasing of photocatalytic activity. Doping has been reported to establish a barrier through equilibration among the photocatalyst and metal deposits and is governed by the difference in work function of the deposits and the electron conduction band of the photocatalyst and does not influence the mechanism of the specific reaction. Doping of a semiconductor such as TiO_2 can be influenced on the band-gap energy and the recombination rate of electron–hole pair [5,6].

ZrO_2 is an *n*-type semiconductor with band-gap energy of 5.0 eV that used as heterogeneous catalyst. The range of band-gap is reported between 3.25 and 5.1 eV depending on the preparation technique of the sample and the most frequent and accepted value is 5.0 eV [7]. The doping of ZrO_2 in lattice of TiO_2 increases the stability of TiO_2 against photocorrosion and decreases the recombination rate of electron–hole pair. The electrons (e^-) and holes (h^+) are the basic species of photocatalytic process in production of active radicals such as $^{\bullet}OH$, $O_2^{-\bullet}$ and $HO_2^{\bullet}$ [8].

Tin(IV) oxide is a semiconductor with band-gap energy of about 3.65 eV at bulk state and is an *n*-type semiconductor crystallizing in tetragonal rutile structure and has been studied as promising semiconductors in the photocatalytic degradation of wastewaters. The doped TiO_2 with Sn^{4+} is due to increasing of lifetime of e^-–h^+ pair [9,10].

The purposes of this work were to synthesize of TiO_2 nanoparticles doped with Zr and Sn as ternary nanocomposite of $Ti_{1-(x+y)}Zr_xSn_yO_2$, characterization of nanocomposites and photocatalytic application of them in photodegradation of tetracycline as a pollutant.

2. Experimental

2.1. Synthesis of nanocomposites

The sol–gel method was used for synthesis of TiO_2 and $Ti_{1-(x+y)}Zr_xSn_yO_2$ nanoparticles. All chemicals were of analytical reagent grade. A certain amount of tetraisopropyl orthotitanate was dissolved in anhydrous ethanol while quickly stirring. Then, a mixture of anhydrous ethanol, distilled water, and acetic acid was added dropwise to titanium solution under stirring. Then, a transparent solution was obtained. After continuous stirring for 60 min at temperature of 60°C, a milky wet gelatin was formed. After aging during 24 h at room temperature, the gelatin was dried in an oven followed by grinding and baking to obtain TiO_2 nanoparticles. Using similar method and with addition given amounts of $ZrCl_4$ and $SnCl_4$ to titanium solution, the $Ti_{0.9}Zr_{0.03}Sn_{0.07}O_2$ (TZ3S7), $Ti_{0.9}Zr_{0.05}Sn_{0.05}O_2$ (TZ5S5), and $Ti_{0.9}Zr_{0.07}Sn_{0.03}O_2$ (TZ7S3) were prepared. The photocatalysts were activated at 600°C and during time of 1.0 h.

2.2. Characterization of nanoparticles

A UV–vis spectrophotometer Cary-100 using a paired 1.0 cm quartz cell was used to record the absorbance spectra of prepared nanocomposites in UV–vis domain. A Diffractometer Bruker D8ADVANCE Germany with anode of Cu ($\lambda = 1.5406$ Å of Cu K_α) and filter of Ni applied to record of X-ray diffraction (XRD) patterns of nanoparticles. The energy dispersive X-ray analysis (EDX) spectra of prepared TZ5S5 nanocomposite were obtained by a Philips XL 30 scanning electron microscope. A JEOL JEM-1200EXII transmission electron microscope (TEM) operating at 120 kV used for estimation of size of TZ5S5 nanoparticles.

2.3. Photodegradation of tetracycline

A photocatalytic reactor with a 36 W mercury low pressure lamp as irradiation source was used to degrade of tetracycline as a pollutant. The light path was 3.0 cm in photoreactor cell. The photoreactor filled with 50 ml of 10–50 mg/L of pollutant, 0.1–1.0 g/L of photocatalysts, pH of 2–9, and irradiation time of 30–180 min. The pH of samples was adjusted with adding of HCl and/or NaOH 0.1 M. The pH of point of zero charge (pH_{PZC}) of heterogeneous catalysts was determined with measurement pH of samples contain 1.0 g/L of catalysts and 0.1 M of NaCl after 24 h of aging. The whole reactor cooled with a water-cooled jacket on its outside, and the temperature was kept at 25°C. All reactants in a degradation reaction were stirred using a magnetic stirrer to uniform of photoreactor cell. In order to setting the adsorption/desorption equilibrium of pollutant on heterogeneous catalysts surface, the reactor was kept in dark conditions within 30 min.

The degradation efficiency (%*D*) of tetracycline was determined with measurement of absorbance of samples by a UV–vis spectrophotometer. The samples centrifuged to remove the heterogeneous photocatalysts before absorbance measurement. The absorbance of samples before (A_o) and after a distinct time (A_t) of irradiation and Beer's law were used for calculate of degradation efficiency (Eq. (1)).

$$\%D = 100 \times [1 - (C_t/C_o)] = 100 \times [1 - (A_t/A_o)] \tag{1}$$

The mineralization of tetracycline in photodegradation process was monitored with TOC/TN analyzer model of Multi N/C 2100, Jena, Germany.

3. Results and discussion

3.1. Characterization of photocatalysts

The XRD patterns of TZ7S3, TZ5S5, and TZ3S7 are indicated in Fig. 1. The XRD patterns show the P25 (anatase–rutile) structure for calcined composites at 600°C. The diffraction peaks at 2θ of 30°, 35°, 42°, 57°, 64°, and 69° confirm the P25 structure [11,12]. Of course, the presence of ZrO_2 and SnO_2 in bulk of TiO_2 nanoparticles is due to a partial distortion in position and overlapping of diffraction peaks vs. reference XRD for P25 structure. This distortion and overlapping is acuter in XRD pattern of A at 2θ of 30° and patterns of B and C at 2θ of 65° in Fig. 1. Due to the difference in ionic radii of zirconium and tin vs. titanium ($Zr^{4+} = 72$ pm, $Sn^{4+} = 71$ pm, and $Ti^{4+} = 61$ pm [13,14]), the doping of them in the structure of TiO_2 can lead to lattice deformations.

Also, the diffraction peaks of ZrO_2 and SnO_2 are not observed in XRD patterns that are attributed to the trace amounts of Zr and Sn in prepared nanocomposites. The average of size of composite nanoparticles (<30 nm) was calculated by the Scherrer formula [15].

Fig. 2 shows the absorbance spectra of prepared nanocomposites. The wavelength of maximum absorbance of TZ3S7, TZ5S5, and TZ7S3 are seen in λ_{max} of 385, 415, and 420 nm, respectively, so that a red-shift is observed vs. TiO_2 nanoparticles ($\lambda_{max} = 378$ nm) [16].

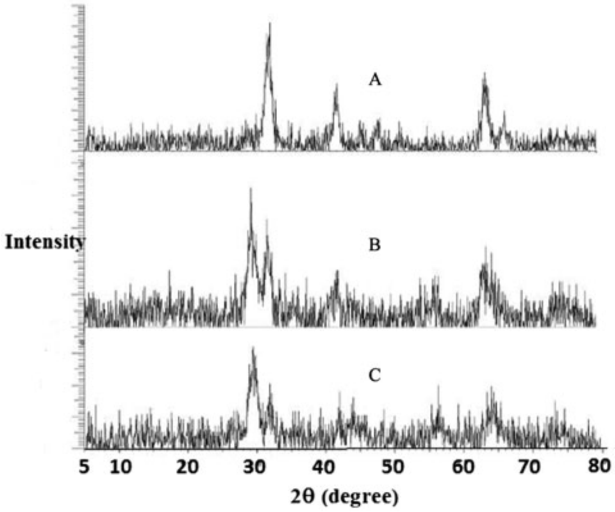

Fig. 1. The XRD patterns of TZ3S7 (A), TZ5S5 (B), and TZ7S3 (C).

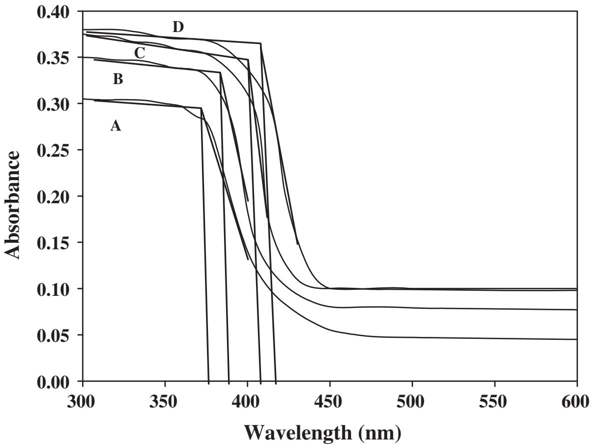

Fig. 2. The absorbance spectra of TiO_2 (A), TZ3S7 (B), TZ5S5 (C), and TZ7S3 (D).

Based on the λ_{max} values, the band-gap energies (E_g) of TZ3S7, TZ5S5, and TZ7S3 are calculated 3.22, 2.99, and 2.95 eV (E_g, eV = 1239.84/λ, nm), respectively. While, the band-gap energy of TiO_2 nanoparticles is obtained 3.28 eV.

The EDX spectra of TZ5S5 nanocomposite is indicated in Fig. 3. The formation of nanocomposite with doped elements of Zr and Sn is approved by the EDX spectra. Also, the TEM images (Fig. 4) show the size of 30–80 nm for prepared nanoparticles of TZ5S5. However, an agglomeration is seen for nanoparticles that are due to a lack of clear image for them.

3.2. Photodegradation of tetracycline

Several kinds of drugs, such as antibiotics, hormones, preservatives, and anesthetics, have been identified in surface water, groundwater, sewage water, and drinking water, of which antibiotics are of special concern due to their extensive use in human and veterinary medicine. Tetracycline is one of the most frequently

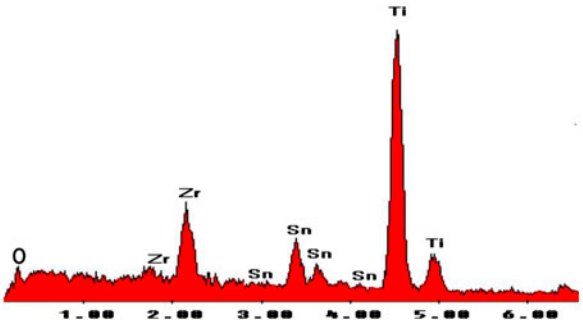

Fig. 3. The EDX spectra of TZ5S5 nanocomposite.

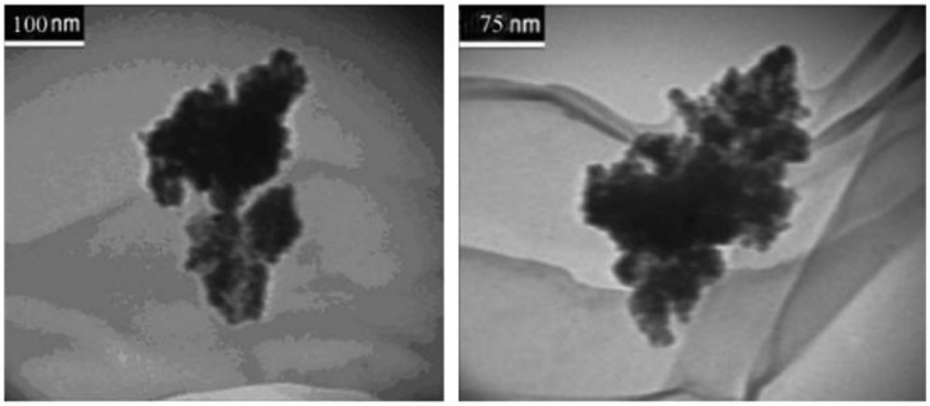

Fig. 4. The TEM images of TZ5S5 nanocomposite.

prescribed groups of antibiotics commonly used as therapeutics and growth promoters in husbandry, cattle, swine, poultry, and fishery, with a widespread presence in surface waters [17,18]. Therefore, degradation of tetracycline as a pollutant using effective, efficient, moderately rate, and relatively inexpensive method can used for treatment of surface waters.

The advance oxidation process at the presence of irradiation and new photocatalysts is used to destruction of tetracycline in aqueous samples. The several parameters including the pH of samples, dose of photocatalyst, irradiation time, and initial concentration of pollutant affect on the degradation efficiency in a photodegradation process [19]. Thus, for arrive to degradation maximum, the optimization of mentioned parameters is the first step in sample treatment.

The pH of samples affect on the surface charge of photocatalysts, the charge of pollutant species, and the surface adsorption of pollutant species. The pH of point of zero charge (pH_{PZC}) is a property of solid particles in aqueous samples. At this pH, the surface charge of solid particles is neutral. The surface charge is positive in $pH < pH_{PZC}$ and negative in $pH > pH_{PZC}$. As seen from Fig. 5, the pH_{PZC} of TZ5S5 nanocomposite as well as the two other prepared nanocomposites is pH 6. Fig. 6 indicates the effect of sample pH on the degradation efficiency of tetracycline. The maximum degradation is obtained in pH 3. The pK_a values of tetracycline molecule are 3.3, 7.68, and 9.7, respectively, for pK_{a1}, pK_{a2}, and pK_{a3} that are related to equilibriums: $TCH_3^+ \leftrightarrow TCH_2$, $TCH_2 \leftrightarrow TCH^-$, and $TCH^- \leftrightarrow TC^{2-}$ [20]. Thus, the dominant species in pH 3 can be the neutral species of TCH_2. The repulsion between the TCH_3^+ species and the positive charge of surface of photocatalysts in pH < 3 is due to decreasing of degradation efficiency. Also, in pH > 7, TCH^- and TC^{2-} species are dominant and the surface of nanocomposite particles has the negative charge. Thus, repulsion between nanocomposite particles and negative species of tetracycline is due to reduction of degradation efficiency [21].

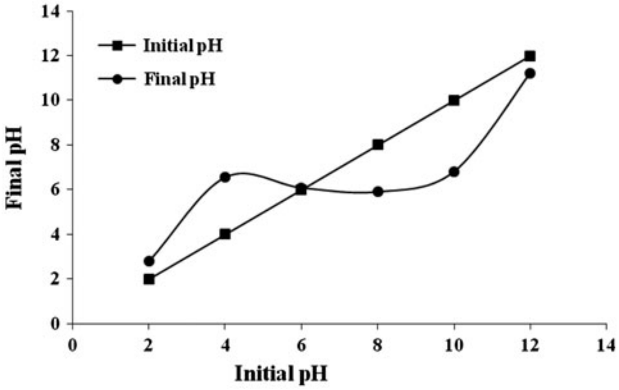

Fig. 5. The pH_{PZC} of TZ5S5 nanocomposite.

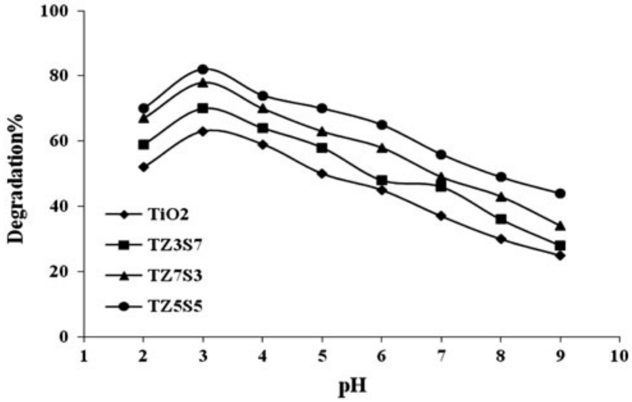

Fig. 6. The effect of sample pH on the degradation efficiency of tetracycline, 1.0 g/L of photocatalyst, 20.0 mg/L of tetracycline, and irradiation time of 180 min.

The first step in photodegradation process is the adsorption of pollutant molecules on the surface of heterogeneous catalyst. The decrease of particles size and increase of amount of catalyst is due to increasing of %*D* of tetracycline. The effect of amount of photocatalysts is shown in Fig. 7. However, the decline of %*D* is observed in amounts of >0.8 g/L of catalyst. The aggregation of nanoparticles and turbidity of aqueous samples can due to decline of degradation efficiency. The penetration of photons is restricted in turbid aqueous samples [22,23].

The kinetic rate constants of photodegradation process of tetracycline catalyzed by prepared photocatalysts are collected in Table 1. The pseudo-first-order rate constants, k_{obs} (min^{-1}), are obtained using Langmuir–Hinshelwood kinetic expression ($\ln(C_o/C_t) = k_{\mathrm{obs}}t$) [24]. The photodegradation conditions are as follows: photocatalyst, 0.8 g/L; pH, 3; initial concentration of tetracycline, 10–50 mg/L; and irradiation time, 30–180 min. The obtained data show the maximum rate of degradation in 20 mg/L of tetracycline. The higher collusion of pollutant molecules with photocatalyst particles is respected with increasing of initial concentration of pollutant. But, in amounts >20 mg/L of pollutant, the competition between the tetracycline and water molecules in adsorption on the surface of catalysts is serious and the decrease of adsorption of water molecules is due to reduction of production of hydroxyl radicals in mechanism of photodegradation [25].

$$\mathrm{TiO_2} + h\nu \rightarrow \mathrm{h}^+ + \mathrm{e}^- \qquad (2)$$

$$\mathrm{h}^+ + \mathrm{H_2O} \rightarrow {}^{\bullet}\mathrm{OH} + \mathrm{H}^+ \qquad (3)$$

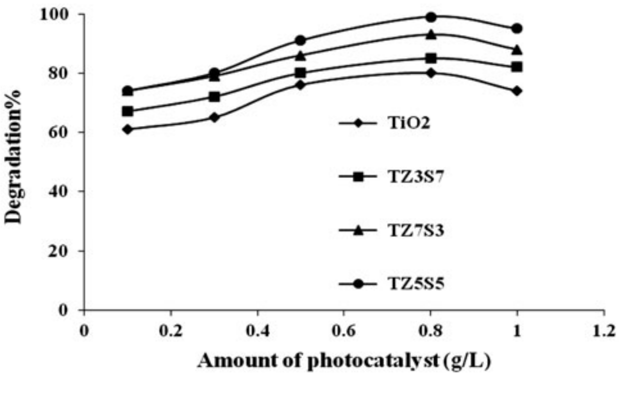

Fig. 7. The effect of photocatalyst dosage on the degradation efficiency of tetracycline, pH 3, 20.0 mg/L of tetracycline, and irradiation time of 180 min.

Also, in higher concentrations of pollutant, to reach photons to catalyst surface is restricted because absorbance of photons by tetracycline molecules.

The order of photocatalytic activity is obtained as follows: TZ5S55 > TZ7S3 > TZ3S7 > $\mathrm{TiO_2}$. Design and preparation of efficient heterogeneous photocatalytic materials still attracts much attention. For this purpose, various methods have been suggested to enhance the photocatalytic activity of $\mathrm{TiO_2}$ (band-gap energy of 3.2 eV), which mainly include doping, functionalization of the surface with metal particles, and reduction of particle size to the nanoscale. Therefore, the band-gap of $\mathrm{TiO_2}$ can decreased and/or recombination of photogenerated electron–hole pairs (e^-–h^+) can prevented effectively. Among these methods, doping of two components into $\mathrm{TiO_2}$ lattice to produce co-doped $\mathrm{TiO_2}$ photocatalysts is one of the most effective ways for enhancing the photocatalytic activity of $\mathrm{TiO_2}$ [26].

The UV–vis spectra of prepared photocatalysts showed the red-shift of band-gap energy of doped $\mathrm{TiO_2}$ versus pure $\mathrm{TiO_2}$. Thus, the efficiency of electron–hole production and the active radicals is increased in photodegradation process. The overlapping of conductance and valance bands of $\mathrm{TiO_2}$, $\mathrm{ZrO_2}$, and $\mathrm{SnO_2}$ semiconductors is due to decrease of band-gap energy. In other words, the reduction of recombination rate of electron–hole is due to addition of lifetime of electrons and holes in conductance and valance bands, respectively. At these conditions, the production efficiency of active radicals such as hydroxyl radical and thus the efficiency of photodegradation are increased [27]. Apparently, the doping of similar amounts of Zr and Sn in $\mathrm{TiO_2}$ is lead to an optimum band-gap in composite photocatalyst. So that, the best rate of photodegradation is obtained at the presence of $\mathrm{Ti_{0.9}Zr_{0.05}Sn_{0.05}O_2}$ (TZ5S5) photocatalyst.

The TOC method was monitored in tetracycline samples (0.2 mg/L) as it decomposed. The results were shown in Fig. 8. After 180 min, TOC of tetracycline in photodegradation reaction at the presence of TZ5S5 photocatalyst was reduced by 90%. The TOC results were also showed the order of photocatalytic activity is as follows: TZ5S5 > TZ7S3 > TZ3S7 > $\mathrm{TiO_2}$.

The reproducibility of photocatalytic activity of TZ5S5 photocatalyst was studied in a four-cycle photodegradation. Each experiment was carried out with 20 mg/L of tetracycline, 0.8 g/L of nanocomposite, pH of 3, and time of 180 min. After each experiment, the catalyst particles was removed, washed with water and ethanol solvent, and dried at 70–80°C temperature, and then used in a new experiment. The degradation was obtained 98, 94, 91, and 85% in four cycles, respectively, that shows the reproducibility

Table 1
The pseudo-first-order rate constants (k_{obs}, min^{-1}) of tetracycline photodegradation at various initial concentrations (mg/L) catalyzed by photocatalysts

Photocatalyst	10	20	30	40	50
TiO_2	$10.1 \pm 0.9 \times 10^{-3}$	$11.2 \pm 1.1 \times 10^{-3}$	$10.4 \pm 0.8 \times 10^{-3}$	$9.3 \pm 1.0 \times 10^{-3}$	$7.8 \pm 1.2 \times 10^{-3}$
$Ti_{0.9}Zr_{0.03}Sn_{0.07}O_2$	$13.8 \pm 1.0 \times 10^{-3}$	$15.2 \pm 0.9 \times 10^{-3}$	$14.1 \pm 1.1 \times 10^{-3}$	$12.7 \pm 1.2 \times 10^{-3}$	$10.4 \pm 1.0 \times 10^{-3}$
$Ti_{0.9}Zr_{0.05}Sn_{0.05}O_2$	$24.3 \pm 1.2 \times 10^{-3}$	$27.0 \pm 1.1 \times 10^{-3}$	$25.2 \pm 1.0 \times 10^{-3}$	$22.1 \pm 1.3 \times 10^{-3}$	$18.9 \pm 0.9 \times 10^{-3}$
$Ti_{0.9}Zr_{0.07}Sn_{0.03}O_2$	$17.6 \pm 1.2 \times 10^{-3}$	$20.6 \pm 1.0 \times 10^{-3}$	$18.4 \pm 0.8 \times 10^{-3}$	$15.2 \pm 1.2 \times 10^{-3}$	$13.5 \pm 1.1 \times 10^{-3}$

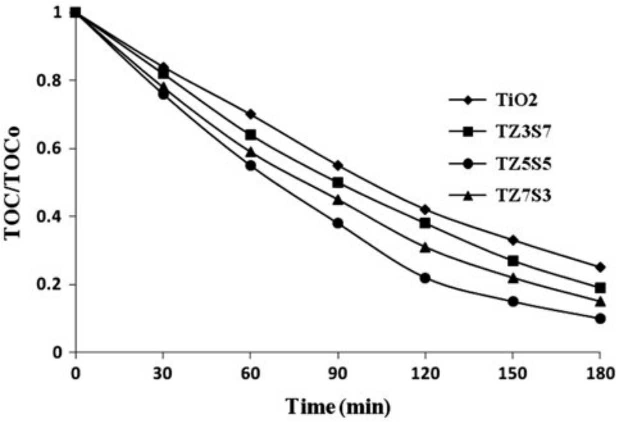

Fig. 8. The TOC variations during the photodegradation of tetracycline catalyzed by different photocatalysts. Initial concentration of tetracycline, 0.2 mg/L; electrolyte and 5 g/L Na_2SO_4.

photocatalytic activity and stability against of photocorrosion.

4. Conclusion

The doped TiO_2 semiconductor with Zr and Sn can increase the photocatalytic activity. The optimized stoichiometry of Zr:Sn:Ti is obtained as 0.05:0.05:0.90, respectively. The $Ti_{0.9}Zr_{0.05}Sn_{0.05}O_2$ nanocomposite can be used as photocatalyst in degradation of tetracycline in aqueous samples.

Acknowledgments

We would like to thank the research committee of Malek-Ashtar University of Technology (MUT) and Islamic Azad University, Shahreza branch for supporting this work.

References

[1] L.F. Liotta, M. Gruttadauria, G. Di Carlo, G. Perrini, V. Librando, Heterogeneous catalytic degradation of phenolic substrates: Catalysts activity, J. Hazard. Mater. 162 (2009) 588–606.

[2] M.R. Hoffmann, S.T. Martin, W. Choi, D.W. Bahnemann, Environmental applications of semiconductor photocatalysis, Chem. Rev. 95 (1995) 69–96.

[3] M.A. Barakat, H. Schaeffer, G. Hayes, S. Ismat-Shah, Photocatalytic degradation of 2-chlorophenol by Co-doped TiO_2 nanoparticles, Appl. Catal. B 57 (2004) 23–30.

[4] T. Kaur, A. Pal Toor, R.K. Wanchoo, Parametric study on degradation of fungicide carbendazim in dilute aqueous solutions using nano TiO_2, Desalin. Water Treat. 54 (2015) 122–131.

[5] H.R. Pouretedal, M. Tavakkoli, Photodegradation of para-nitrophenol catalyzed by Fe_2O_3/FeS nanocomposite, Desalin. Water Treat. 51 (2013) 4744–4749.

[6] A. Bansal, S. Madhavi, T.T.Y. Tan, T.M. Lim, Effect of silver on the photocatalytic degradation of humic acid, Catal. Today 131 (2008) 250–254.

[7] I.A. Salem, Kinetics and mechanism of the color removal from congo red with hydrogen peroxide catalyzed by supported zirconium oxide, Transition Metal Chem. 25 (2000) 599–604.

[8] C. Karunakaran, S. Senthilvelan, Photocatalysis with ZrO_2: Oxidation of aniline, J. Mol. Catal. A 233 (2005) 1–8.

[9] M. Zhang, T. An, X. Hu, C. Wang, G. Sheng, J. Fu, Preparation and photocatalytic properties of a nanometer ZnO–SnO_2 coupled oxide, Appl. Catal. A 260 (2004) 215–222.

[10] H.R. Pouretedal, A. Shafeie, M.H. Keshavarz, Preparation, characterization and catalytic activity of tin dioxide and zero-valent tin nanoparticles, J. Korean Chem. Soc. 56 (2012) 484–490.

[11] M. Nikazar, Kh. Gholivand, K. Mahanpoor, Photocatalytic degradation of Acid Red 114 in water with TiO_2 supported on clinoptilolite as a catalyst, Desalination 219 (2008) 29–35.

[12] L. Gomathi Devi, B. Narasimha Murthy, S. Girish Kumar, Heterogeneous photocatalytic degradation of anionic and cationic dyes over TiO_2 and TiO_2 doped with Mo^{6+} ions under solar light: Correlation of dye structure and its adsorptive tendency on the degradation rate, Chemosphere 76 (2009) 1163–1166.

[13] Z. Xiufeng, L. Juan, L. Lianghai, W. Zuoshan, Preparation of crystalline Sn-doped TiO_2 and its application in visible-light photocatalysis, J. Nanomater. 2011 (2011) 1–5.

[14] C. Tiejun, L. Yuchao, P. Zhenshan, L. Yunfei, W. Zongyuan, D. Qian, Photocatalytic performance of TiO_2 catalysts modified by $H_3PW_{12}O_{40}$, ZrO_2 and CeO_2, J. Environ. Sci. 21 (2009) 997–1004.

[15] H.R. Pouretedal, M. Kiyani, Photodegradation of 2-nitrophenol catalyzed by CoO, CoS and CoO/CoS nanoparticles, J. Iran. Chem. Soc. 11 (2014) 271–277.

[16] X.D. Zhu, Y.J. Wang, R.J. Sun, D.M. Zhou, Photocatalytic degradation of tetracycline in aqueous solution by nanosized TiO_2, Chemosphere 92 (2013) 925–932.

[17] J. Bai, Y. Liu, J. Li, Ba. Zhou, Q. Zheng, W. Cai, A novel thin-layer photoelectrocatalytic (PEC) reactor with double-faced titania nanotube arrays electrode for effective degradation of tetracycline, Appl. Catal. B 98 (2010) 154–160.

[18] S. Yahiat, F. Fourcade, S. Brosillon, A. Amrane, Removal of antibiotics by an integrated process coupling photocatalysis and biological treatment—Case of tetracycline and tylosin, Int. Biodet. Biodeg. 65 (2011) 997–1003.

[19] Y. Du, M. Qiu, Comparative study of advanced oxidation for textile wastewater, Desalin. Water Treat. 51 (2013) 5954–5958.

[20] C.V. Gómez-Pacheco, M. Sánchez-Polo, J. Rivera-Utrilla, J.J. López-Peñalver, Tetracycline degradation in aqueous phase by ultraviolet radiation, Chem. Eng. J. 187 (2012) 89–95.

[21] H.R. Pouretedal, H. Eskandari, M.H. Keshavarz, A. Semnani, Photodegradation of organic dyes using nanoparticles of cadmium sulfide doped with manganese, nickel and copper as nanophotocatalyst, Acta Chim. Slov. 56 (2009) 353–361.

[22] M. Riazian, A. Bahari, Effect of sol concentration on the nanostructural characterization of TiO_2–Al_2O_3–SiO_2 compounds, J. Nano. Mater. 81 (2011) 1904–1907.

[23] A. Nezamzadeh-Ejhieh, Z. Salimi, Heterogeneous photodegradation catalysis of o-phenylenediamine using CuO/X zeolite, Appl. Catal. A 390 (2010) 110–118.

[24] A. Rao, B. Sivasankar, V. Sadasivam, Kinetic studies on the photocatalytic degradation of Direct Yellow 12 in the presence of ZnO catalyst, J. Mol. Catal. A: Chem. 306 (2009) 77–81.

[25] M. Movahedi, A.R. Mahjoub, S. Janitabar-Darzi, Photodegradation of Congo red in aqueous solution on ZnO as an alternative catalyst to TiO_2, J. Iran. Chem. Soc. 6 (2009) 570–577.

[26] M. Behpour, S.M. Ghoreishi, F.S. Razavi, Photocatalytic activy of TiO_2/Ag nanoparticle on degradation of water pollution, J. Nanomater. Biostruct. 5 (2010) 467–475.

[27] H.R. Pouretedal, M.H. Keshavarz, M.H. Yosefi, A. Shokrollahi, A. Zali, Photodegradation of HMX and RDX in the presence of nanocatalyst of zinc sulfide doped with copper, Iran. J. Chem. Chem. Eng. 28 (2009) 13–20.